



# Fe<sub>3</sub>O<sub>4</sub>@graphene oxide composite: A magnetically separable and efficient catalyst for the reduction of nitroarenes

Guangyu He<sup>a,b</sup>, Weifeng Liu<sup>a</sup>, Xiaoqiang Sun<sup>a</sup>, Qun Chen<sup>a,\*</sup>, Xin Wang<sup>b</sup>, Haiqun Chen<sup>a,\*</sup>

<sup>a</sup>Jiangsu Key Laboratory of Advanced Catalytic Materials and Technology, Changzhou University, Jiangsu Province, Changzhou 213164, China

<sup>b</sup>Key Laboratory of Ministry of Education for Soft Chemistry and Functional Materials, Nanjing University of Science and Technology, Nanjing 210094, China

## ARTICLE INFO

### Article history:

Received 7 November 2012

Received in revised form 11 January 2013

Accepted 12 January 2013

Available online 24 January 2013

### Keywords:

A. Composites

A. Magnetic materials

D. Catalytic properties

## ABSTRACT

We reported a facile co-precipitation method to prepare a highly active Fe<sub>3</sub>O<sub>4</sub>@graphene oxide (Fe<sub>3</sub>O<sub>4</sub>@GO) composite catalyst, which was fully characterized by means of X-ray diffraction (XRD), Fourier transformed infrared (FTIR) spectroscopy, transmission electron microscopy (TEM) and N<sub>2</sub> adsorption–desorption measurements. The results demonstrated that the Fe<sub>3</sub>O<sub>4</sub> nanoparticles (Fe<sub>3</sub>O<sub>4</sub> NPs) with a small diameter of around 12 nm were densely and evenly deposited on the graphene oxide (GO) sheets. The as-prepared Fe<sub>3</sub>O<sub>4</sub>@GO composite was explored as a catalyst to reduce a series of nitroarenes for the first time, which exhibited a great activity with a turnover frequency (TOF) of 3.63 min<sup>-1</sup>, forty five times that of the commercial Fe<sub>3</sub>O<sub>4</sub> NPs. The dosages of catalyst and hydrazine hydrate are both less than those reported. Furthermore, the composite catalyst can be easily recovered due to its magnetic separability and high stability.

© 2013 Elsevier Ltd. All rights reserved.

## 1. Introduction

Aromatic amines are important organic compounds which are widely used as key intermediates in dye, pharmaceutical and pesticide industry [1]. At present, aromatic amines are generally prepared from the corresponding aromatic nitro compounds by a catalytic reduction or a non-catalytic process. The conventional non-catalytic method mainly uses metal/acid [2] or sodium sulfide [3] reduction, which presents difficulties in product isolation and has low reduction efficiency. Moreover, it is accompanied by serious waste pollution. Therefore, an increasing number of researchers have shifted their attention to catalytic reduction because of its better product quality and less pollution.

So far, the catalysts used for the catalytic reduction of nitro compounds give priority to the precious metals [4–8], such as Pd and Pt, which are expensive and usually sensitive to both air and moisture. Another type of catalyst is the iron-based compounds, including FeCl<sub>3</sub> [9], iron oxides [10] and FeOOH [11], which are mainly explored for the reduction of nitroarenes in the presence of hydrazine. They are generally cheaper, but their catalytic activities are not desirable. More recently, the iron (II) salt/iron phthalocyanine [12], iron-phenanthroline/C [13] and nickel–iron mixed oxide [14] have been exploited as catalysts for the reduction of

nitroarenes on account of their high catalytic performance and selectivity, where some unsaturated groups including –C=C–, –CN and –COOR located in the side chain of the benzene ring are not influenced by the catalyst. However, there are some disadvantages associated with these Fe-based catalysts, such as a complicated preparation process, high cost, and/or difficult catalyst separation. To overcome the problem of catalyst separation, the magnetic separation has been utilized. Kim et al. [15] prepared magnetically recyclable Rh-Fe<sub>3</sub>O<sub>4</sub> heterostructured NPs, which exhibited good catalytic activity towards the reduction of nitroarenes. Afterwards, they accomplished an efficient and selective nitro group reduction using commercially available Fe<sub>3</sub>O<sub>4</sub> NPs [16] (<50 nm), which yielded up to 99% of aniline within 45 min with 37.6 wt% catalyst used. However, the same reaction employing 1.8 wt% Fe<sub>3</sub>O<sub>4</sub> NPs gave only an 11% yield after 6 h. Therefore, it is of great importance to extend the method of the catalytic reduction of nitroarenes for industrial application by preparing magnetically separable Fe<sub>3</sub>O<sub>4</sub> NPs with high catalytic activity.

Recently, we reported the synthesis of several magnetically separable metal oxide-graphene composites [17,18] with superior catalytic oxidation performance due to the synergistic effect between the metal oxides and graphene. On the basis of these researches, we prepared a magnetically separable Fe<sub>3</sub>O<sub>4</sub>@graphene oxide (Fe<sub>3</sub>O<sub>4</sub>@GO) composite through one-step co-precipitation, which was proved to be an excellent catalyst for the reduction of nitrobenzene in the presence of hydrazine. Moreover, the composite was easily recoverable with good cycle stability and showed high catalytic activity for the reduction of some other nitroarenes as well.

\* Corresponding authors. Tel.: +86 519 86330233; fax: +86 519 86330233.

E-mail addresses: [chenqunjpu@yahoo.com](mailto:chenqunjpu@yahoo.com) (Q. Chen), [hqchenyf@hotmail.com](mailto:hqchenyf@hotmail.com) (H. Chen).

## 2. Experimental

### 2.1. Materials

Natural graphite powder (99.9%, 500 mesh),  $\text{FeCl}_3 \cdot 6\text{H}_2\text{O}$ ,  $\text{FeSO}_4 \cdot 7\text{H}_2\text{O}$ , ammonia (22–28%), hydrazine hydrate (80%), nitrobenzene, *o*-nitrotoluene, *o*-, *m*-, *p*-nitroaniline and other materials were purchased from Sinopharm Chemical Reagent Co., Ltd. (China). All chemicals were of analytical grade and used as received.

### 2.2. Preparation of $\text{Fe}_3\text{O}_4$ @GO composite

Graphite oxide was synthesized using a modified Hummers method [19,20] and exfoliated to afford an aqueous dispersion of graphene oxide (GO) under ultrasonication.  $\text{Fe}_3\text{O}_4$ @GO composites with different  $\text{Fe}_3\text{O}_4$  to GO mass ratios (2, 5, 10, 15 and 20, respectively) were synthesized. Taken as an example, the  $\text{Fe}_3\text{O}_4$ @GO composite with  $\text{Fe}_3\text{O}_4$  to GO mass ratio of 10 was synthesized as follows. 15 mL of GO ( $2.72 \text{ mg mL}^{-1}$ ) was dispersed into 40 mL ethanol with stirring. 0.9522 g of  $\text{FeCl}_3 \cdot 6\text{H}_2\text{O}$  (3.5228 mmol) and 1.0520 g of  $\text{FeSO}_4 \cdot 7\text{H}_2\text{O}$  (3.7842 mmol) were dissolved in 10 mL of distilled water under sonication, then the solution was injected dropwise into the GO suspension and stirred for 30 min. The resulting mixture was heated to 68 °C before ammonia solution was added to adjust the pH to 10. The mixture was stirred at 68 °C for 2 h and then cooled to room temperature. The  $\text{Fe}_3\text{O}_4$ @GO composite was separated from the mixture using a permanent magnet, and rinsed three times with ethanol and distilled water respectively before being dried at 65 °C for 12 h. For comparison, the bare  $\text{Fe}_3\text{O}_4$  NPs were prepared following the same procedure in the absence of GO.

### 2.3. Characterization

X-ray diffraction (XRD) measurements were carried out using a Bruker D8 Advance diffractometer with  $\text{Cu-K}\alpha$  radiation ( $\lambda = 1.54 \text{ \AA}$ ). FTIR spectra were recorded on a Nicolet 370 FT/IR spectrometer (Thermo Nicolet, USA) using pressed KBr pellets. Transmission electron microscopy (TEM) images were taken with a JEOL JEM-2100 microscope (JEOL, Japan). The BET surface area of the as-synthesized samples was measured using an ASAP2010 C surface aperture adsorption instrument (Micromeritics Instrument Corporation, USA) by  $\text{N}_2$  physisorption at 77 K. The reaction process was monitored using an Agilent 6890N gas chromatography equipped with an FID detector (Agilent, USA). The product was analyzed using an Agilent 6890N/5973N GC-MS (Agilent, USA).

### 2.4. Catalytic reduction of nitroarenes over $\text{Fe}_3\text{O}_4$ @GO composite

A mixture of an aromatic nitro compound (e.g., nitrobenzene, 2.4600 g, 20 mmol), ethanol (12 mL) and as-prepared  $\text{Fe}_3\text{O}_4$ @GO composite (0.0773 g, 3.1 wt% of nitrobenzene) was heated to reflux with stirring, followed by dropwise addition of hydrazine hydrate (72 mmol, 3.6 equiv.). The reaction mixture was kept at reflux with stirring and the reaction progress was monitored by gas chromatography. The  $\text{Fe}_3\text{O}_4$ @GO composite was separated by applying an external magnetic field at the end of the reaction and washed with ethanol three times before being vacuum dried. Then, the composite was weighed and recycled for the reduction reaction. Quantitative and qualitative analyses of the reactions were performed using GC and GC-MS, and the products were identified by comparison with authentic samples.

## 3. Results and discussion

### 3.1. Characterization of $\text{Fe}_3\text{O}_4$ @GO composite

The phase structure of the sample was obtained through X-ray diffraction (XRD) measurement. As shown in Fig. 1, the original GO exhibits a sharp peak at  $2\theta = 11.2^\circ$ , which can be ascribed to the (0 0 1) plane of GO. However, no diffraction peak of GO is observable for the as-prepared  $\text{Fe}_3\text{O}_4$ @GO composite, suggesting that the layer stacking of the GO sheets was destroyed by the loading of  $\text{Fe}_3\text{O}_4$  NPs. The diffraction peaks at  $2\theta = 30.18^\circ$ ,  $35.52^\circ$ ,  $43.36^\circ$ ,  $53.70^\circ$ ,  $57.30^\circ$  and  $62.78^\circ$  can be indexed to (2 2 0), (3 1 1), (4 0 0), (4 2 2), (5 1 1) and (4 4 0) planes of cubic  $\text{Fe}_3\text{O}_4$  (JCPDS 89-2355). The broad diffraction peaks indicate a small size of the  $\text{Fe}_3\text{O}_4$  NPs, which is about 11.2 nm according to the Scherrer equation.

The FTIR spectra of GO and the  $\text{Fe}_3\text{O}_4$ @GO composite are shown in Fig. 2. As expected, the FTIR spectrum of GO is in good agreement with previous works [21,22]. The broad and intense band observed at  $3402 \text{ cm}^{-1}$  is ascribed to the stretching vibration of O–H. The band at  $1090$ ,  $1380$  and  $1716 \text{ cm}^{-1}$  corresponds to the C–O stretching vibration, the C–O–H deformation vibration, and the C=O stretching vibration, respectively. The peak at  $1618 \text{ cm}^{-1}$  can be assigned to the aromatic skeletal C=C stretching vibration of the unoxidized graphitic domains. Compared with that of GO, a new prominent absorption band appeared at about  $580 \text{ cm}^{-1}$  in the FTIR spectrum of the  $\text{Fe}_3\text{O}_4$ @GO composite, which corresponds to the stretching mode of Fe–O [23].

The TEM image of the  $\text{Fe}_3\text{O}_4$ @GO composite (Fig. 3) showed that the GO sheets with a lateral dimension of about  $1 \mu\text{m}$  were decorated with large quantity of  $\text{Fe}_3\text{O}_4$  NPs. The transparency of the GO sheet indicated that the graphite oxide was well exfoliated into few-layer GO sheets. As shown in the inset (a) of Fig. 3, a narrow size distribution of  $\text{Fe}_3\text{O}_4$  NPs was obtained with a mean size of around 12 nm, which is in accordance with the XRD result. The homogeneous distribution of the  $\text{Fe}_3\text{O}_4$  NPs was expected to offer an enhanced catalytic activity. The crystal lattice fringes with *d*-spacing of 0.25 nm (inset b of Fig. 3) can be assigned to the (3 1 1) plane of  $\text{Fe}_3\text{O}_4$ .

$\text{N}_2$  adsorption–desorption isotherms were conducted to investigate the porous structure and surface area of the bare  $\text{Fe}_3\text{O}_4$  NPs and the  $\text{Fe}_3\text{O}_4$ @GO composite. As shown in Fig. 4, the surface area of the  $\text{Fe}_3\text{O}_4$ @GO composite calculated by the Brunauer–Emmett–Teller method is  $137 \text{ m}^2 \text{ g}^{-1}$ , which is much higher than that of the bare  $\text{Fe}_3\text{O}_4$  NPs ( $58 \text{ m}^2 \text{ g}^{-1}$  as shown in Fig. S1). The  $\text{N}_2$  isotherm of the  $\text{Fe}_3\text{O}_4$ @GO composite is close to Type IV with an evident hysteresis loop in the 0.4–1.0 range of low relative pressure, indicating that the existence of GO prevented the  $\text{Fe}_3\text{O}_4$  NPs from

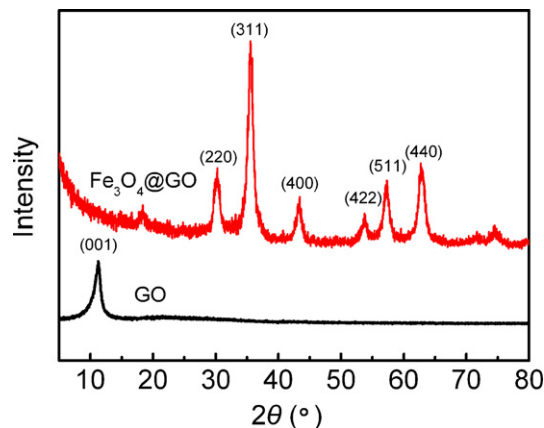


Fig. 1. XRD patterns of GO and  $\text{Fe}_3\text{O}_4$ @GO composite.

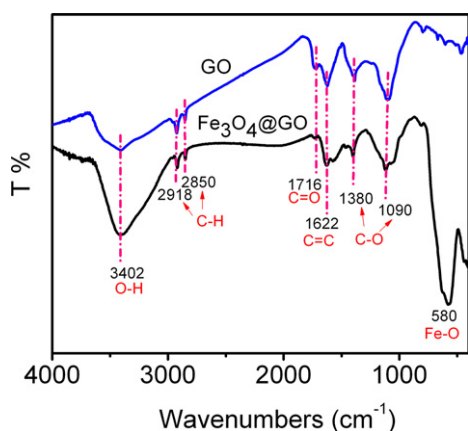


Fig. 2. FTIR spectra of GO and  $\text{Fe}_3\text{O}_4$ @GO composite.

aggregating, which was expected to improve the catalytic activity of the  $\text{Fe}_3\text{O}_4$ @GO composite.

### 3.2. The catalytic performance of the $\text{Fe}_3\text{O}_4$ @GO composite for the catalytic reduction of nitrobenzene

#### 3.2.1. The activity comparison of different reaction systems

Reduction of nitrobenzene with hydrazine was carried out respectively in the absence of a catalyst, the presence of bare  $\text{Fe}_3\text{O}_4$  NPs, and the presence of  $\text{Fe}_3\text{O}_4$ @GO composite to investigate the catalytic effect of the as-prepared  $\text{Fe}_3\text{O}_4$ @GO composite on the reaction. As shown in Fig. 5, no appreciable reaction took place after 18 min without a catalyst. About 15% of nitrobenzene remained unreduced after 18 min with bare  $\text{Fe}_3\text{O}_4$  NPs employed as the catalyst. But when the  $\text{Fe}_3\text{O}_4$ @GO composite was used as the catalyst, the reaction proceeded much faster and completed in 18 min.

In addition, the as-prepared  $\text{Fe}_3\text{O}_4$ @GO composite showed a higher TOF (Table S1) of  $3.63 \text{ min}^{-1}$  than that of the commercial  $\text{Fe}_3\text{O}_4$  NPs, suggesting that the dispersion of the  $\text{Fe}_3\text{O}_4$  NPs on GO sheets enhanced the catalytic property. Though the bare  $\text{Fe}_3\text{O}_4$  NPs also presented good catalytic activity, they were prone to

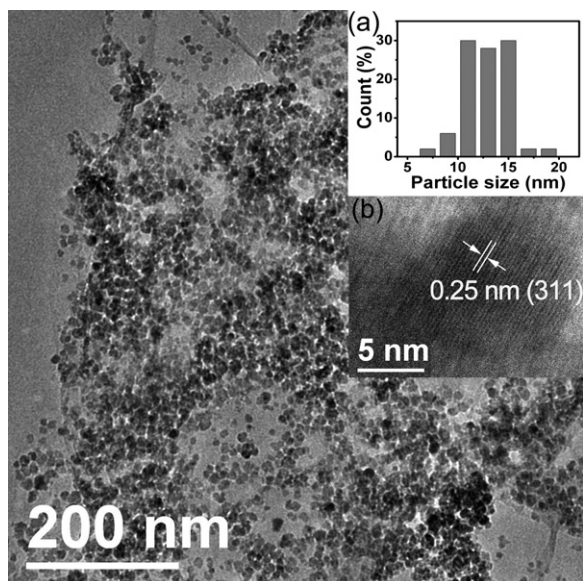


Fig. 3. TEM image of  $\text{Fe}_3\text{O}_4$ @GO composite. The inset (a) and (b) is the size distribution histogram and a high resolution TEM image of  $\text{Fe}_3\text{O}_4$  NPs, respectively.

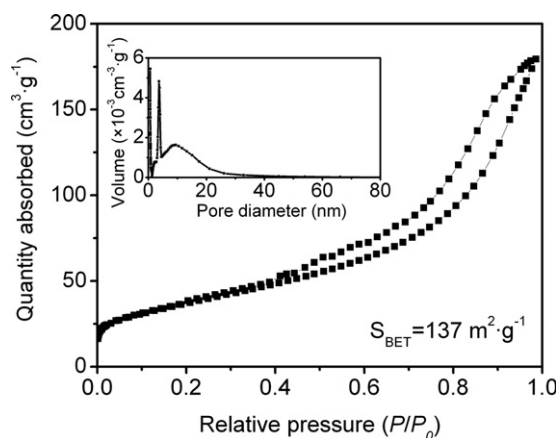


Fig. 4. Nitrogen adsorption–desorption isotherms for  $\text{Fe}_3\text{O}_4$ @GO composite. The inset image shows the pore size distribution for  $\text{Fe}_3\text{O}_4$ @GO composite.

aggregate. After the hybridization of  $\text{Fe}_3\text{O}_4$  NPs and GO, the surface energy of  $\text{Fe}_3\text{O}_4$  NPs decreased since the oxygen-containing functional groups on the GO sheets acted as anchoring sites for  $\text{Fe}_3\text{O}_4$  NPs, which is beneficial to the well distribution of the nanoparticles. Moreover, GO sheets with large surface area had excellent adsorption ability for organic compounds, which increased the collision probability between the catalyst and the reaction reagents. In other words, the  $\text{Fe}_3\text{O}_4$ @GO composite gained enhanced properties due to the synergistic effects between the GO sheets and the  $\text{Fe}_3\text{O}_4$  NPs.

#### 3.2.2. The effect of the composition of $\text{Fe}_3\text{O}_4$ @GO composite on the activity of the catalyst

We found that the mass ratio of  $\text{Fe}_3\text{O}_4$  to GO in the  $\text{Fe}_3\text{O}_4$ @GO composite played a very important role in the catalytic activity. As shown in Fig. 6, after the same reaction time (18 min), the yield of aniline increased gradually with the increase of the mass ratio of  $\text{Fe}_3\text{O}_4$  to GO. When the mass ratio of  $\text{Fe}_3\text{O}_4$  to GO was increased to 10, a maximum yield of 99.2% was obtained. Further increase of the load of  $\text{Fe}_3\text{O}_4$  did not afford significant benefits in terms of the reaction yield. It might be because increasing the mass ratio of  $\text{Fe}_3\text{O}_4$  to GO enhanced the effective contact between the molecules of nitroarenes and the active sites of catalyst. However, when the mass ratio of  $\text{Fe}_3\text{O}_4$  to GO was increased over a certain value, overly covered surface of GO sheets might hinder the chemical adsorption of nitroarenes onto GO through  $\pi$ - $\pi$  stacking [24], which went against the reduction reaction. The optimal mass ratio ( $\text{Fe}_3\text{O}_4/\text{GO} = 10$ ) was applied to the subsequent experiments unless specifically stated.

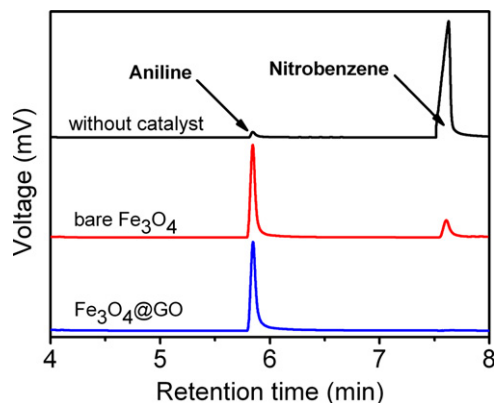


Fig. 5. GC analyses of the reduction of nitrobenzene in different reaction systems after 18 min.

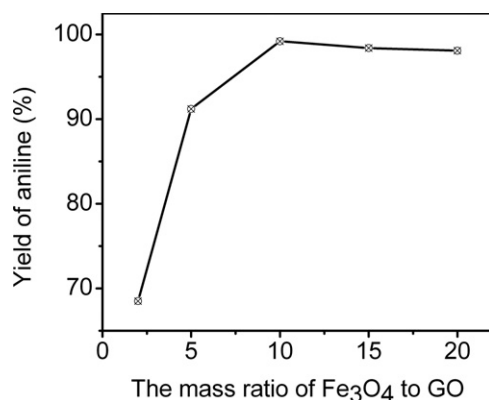


Fig. 6. The effect of the mass ratio of Fe<sub>3</sub>O<sub>4</sub> to GO (2, 5, 10, 15 and 20, respectively) in the Fe<sub>3</sub>O<sub>4</sub>@GO composite on the activity of the catalyst.

### 3.2.3. The effect of the catalyst dosage on the reduction reaction

Table 1 shows the impact of different dosages of Fe<sub>3</sub>O<sub>4</sub>@GO composite on the reduction of nitrobenzene. When the amount of Fe<sub>3</sub>O<sub>4</sub>@GO was 1.2 wt%, the yield of amine reached 98.5% within 35 min. The reaction proceeded faster with larger amount of catalyst, which was contributed to the proportional increase in the number of active catalytic sites. That is to say, with increasing the dosage of Fe<sub>3</sub>O<sub>4</sub>@GO composite, more and more active sites were available to accelerate the decomposition of hydrazine, thus increasing the utilization of hydrazine and promoting the rate of reaction. Compared with the reported catalyst dosage, such as 160.0 mg of MgO–Fe<sub>2</sub>O<sub>3</sub> towards 8.1 mmol of nitrobenzene [25], and 150.0 mg of Ni–Fe oxide towards 4.1 mmol of nitrobenzene [14], the introduction of GO in the Fe<sub>3</sub>O<sub>4</sub>@GO composite as a carrier to support the Fe<sub>3</sub>O<sub>4</sub> NPs not only shortened the reaction time but also decreased the catalyst dosage greatly, indicating that the performance of the nanoparticles was greatly improved.

### 3.2.4. The effect of hydrazine hydrate dosage and reaction temperature on the reaction

As is well known, being a two-electron reducing agent [26], hydrazine provides the hydrogen source for the reduction of nitrobenzene. The reduction of nitrobenzene over the Fe<sub>3</sub>O<sub>4</sub>@GO composite followed a redox mechanism [27,28], in which the catalyst was reduced by hydrazine and re-oxidized by the nitrobenzene. Fe<sup>3+</sup> was reduced by hydrazine to Fe<sup>2+</sup> while the hydrazine decomposed to N<sub>2</sub> and H<sup>+</sup>. The nitrobenzene was reduced to aniline by Fe<sup>2+</sup> and H<sup>+</sup>, while Fe<sup>2+</sup> was oxidized to Fe<sup>3+</sup>.

The impact of the dosage of hydrazine hydrate on the catalytic effect was investigated with the solvent and the reaction temperature fixed (i.e. reflux in ethanol). The results listed in entries 1–5 of Table 2 show that both the reaction rate and the yield of aniline increased with increasing the dosage of hydrazine hydrate. The “Time” listed in Table 2 was the reaction duration traced by the gas chromatography when the starting material nitrobenzene was converted completely and the yield of the aniline did not increase any more, which illustrated the reaction rate. Considering the production cost in industrial application of this work, 3.6 equiv. of hydrazine hydrate was chosen as the

Table 1  
Reaction dependence on the amount of Fe<sub>3</sub>O<sub>4</sub>@GO composite.

Entry	Amount of Fe <sub>3</sub> O <sub>4</sub> @GO (wt%)	Time (min)	Yield of aniline (%)
1	1.2	35	98.5
2	2.0	24	98.7
3	3.1	18	99.2

Table 2

The effect of hydrazine hydrate dosage and reaction temperature on the reduction reaction.

Entry	N <sub>2</sub> H <sub>4</sub> ·H <sub>2</sub> O	Solvent	Time (min)	Yield of aniline (%)
1	1.5 equiv.	EtOH	60	80.1
2	2.0 equiv.	EtOH	30	98.5
3	3.0 equiv.	EtOH	20	98.8
4	3.6 equiv.	EtOH	18	99.2
5	4.0 equiv.	EtOH	17	99.3
6	3.6 equiv.	EtOH	60 <sup>a</sup>	7.1
7	3.6 equiv.	Toluene	10 <sup>b</sup>	98.3
8	3.6 equiv.	Isopropanol	15	98.1
9	3.6 equiv.	Tetrahydrofuran	40	96.4
10	3.6 equiv.	Dichloromethane	60	39.8

<sup>a</sup> Reaction temperature: room temperature.

<sup>b</sup> Reaction temperature: 98 °C.

optimal value after repeated experiments and applied to the subsequent experiments.

Then we studied the impact of the reaction temperature on the catalytic effect. The reaction was carried out in ethanol solvent under reflux and at room temperature, respectively. The Fe<sub>3</sub>O<sub>4</sub>@GO composite exhibited an extremely higher catalytic activity at reflux temperature (shown in entry 4 of Table 2) than at room temperature (shown in entry 6 of Table 2), suggesting that higher reaction temperature is conducive to the catalytic reduction.

The catalytic effect of the Fe<sub>3</sub>O<sub>4</sub>@GO composite was also explored in different solvent under reflux unless specifically stated. The results listed in entries 7–10 of Table 2 indicated that the Fe<sub>3</sub>O<sub>4</sub>@GO composite exhibited excellent performance in toluene or isopropanol solvent as well, suggesting the as-prepared catalyst is generally applicable in certain kinds of solvents.

### 3.2.5. The cycle stability of the Fe<sub>3</sub>O<sub>4</sub>@GO composite

Although the Fe<sub>3</sub>O<sub>4</sub>@GO composite exhibited a high catalytic activity, in view of practical applications, it is of great significance to investigate the cycle stability of the Fe<sub>3</sub>O<sub>4</sub>@GO composite. Therefore, the Fe<sub>3</sub>O<sub>4</sub>@GO composite was separated magnetically (Fig. S2) and recycled in the reduction of nitrobenzene to evaluate its recycling performance. As shown in Fig. 7, no appreciable loss of catalytic activity was observed after the Fe<sub>3</sub>O<sub>4</sub>@GO composite was recycled for several times, indicating very high stability of the Fe<sub>3</sub>O<sub>4</sub>@GO composite.

It is worth noting that though the FTIR spectra of the catalyst (Fig. S3) showed the GO in the Fe<sub>3</sub>O<sub>4</sub>@GO composite was reduced by hydrazine simultaneously during the first cycle of the catalytic reduction of nitrobenzene, no obvious further change was found after the recycling. In addition, the XRD patterns (Fig. S4) and TEM

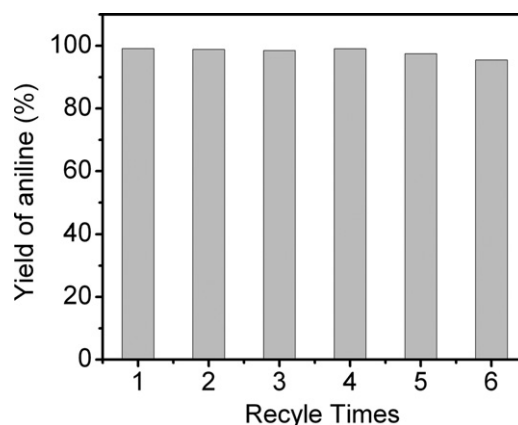


Fig. 7. Reusability of the Fe<sub>3</sub>O<sub>4</sub>@GO composite for nitrobenzene reduction (the reaction of the first recycling completed in 18 min, while the reaction of the following recycling completed in 20 min).

**Table 3**Reduction of other nitroarenes over Fe<sub>3</sub>O<sub>4</sub>@GO composite.

Entry	substrate	product	Time (min)	Yield (%)	Reference <sup>a</sup>	
					Time (min)	Yield (%)
1			40	98.8	116	99
2			45	97.5	112	98
3			80	97.1	109	99
4			95	82.5	142	97
5			20	99.2		

<sup>a</sup> Reaction conditions: 0.5 g of aromatic nitro compound, 1 mL of hydrazine hydrate, 0.15 g of nickel–iron mixed oxide and 15 mL of propan-2-ol under reflux.

images (Fig. S5) proved that the cubic crystal structure and the morphology of Fe<sub>3</sub>O<sub>4</sub> NPs on the GO sheets remain unchanged after the recycling. Moreover, the magnetically separated Fe<sub>3</sub>O<sub>4</sub>@GO was weighed during the recycling with no obvious mass loss observed, demonstrating that the Fe<sub>3</sub>O<sub>4</sub>@GO composite is stable for recycling.

### 3.3. The catalytic effect of the Fe<sub>3</sub>O<sub>4</sub>@GO composite on other nitro compounds

We also employed the Fe<sub>3</sub>O<sub>4</sub>@GO composite to catalyze the reductions of some nitro compounds other than nitrobenzene, which showed superior catalytic activity as well. As shown in Table 3, the Fe<sub>3</sub>O<sub>4</sub>@GO composite was found to be able to catalyze the reduction of 2-nitro-6-chlorotoluene completely within 20 min. When *o*-nitrotoluene or *o*-nitroaniline was used as the starting material, a high yield of product was obtained within a short reaction time. The dosages of Fe<sub>3</sub>O<sub>4</sub>@GO (3.1 wt%) and hydrazine hydrate (3.6 equiv.) were less than those reported, e.g., nickel–iron mixed oxides (30.0 wt%) and hydrazine hydrate (5.0 equiv.) [14]. Three reasons might contribute to the excellent performance of the Fe<sub>3</sub>O<sub>4</sub>@GO composite. First, the oxygen-containing groups on the GO sheets provided the anchoring sites for the deposition of Fe<sub>3</sub>O<sub>4</sub> NPs, which enabled Fe<sub>3</sub>O<sub>4</sub> NPs to distribute evenly on the surface of GO thus avoiding their aggregation. Second, nitroarenes can be adsorbed onto GO through  $\pi$ – $\pi$  stacking interactions, which increased the effective contact between the molecules of nitro compounds and the Fe<sub>3</sub>O<sub>4</sub> NPs. Third, the carbon atoms at the zigzag edges of the graphene interacted with the terminal oxygen atoms of the nitroarenes, thereby weakening the N–O bonds for effective reduction [29].

## 4. Conclusions

In summary, a magnetic Fe<sub>3</sub>O<sub>4</sub>@GO composite was prepared by a facile co-precipitation method. The presence of GO prevented the

Fe<sub>3</sub>O<sub>4</sub> NPs from aggregating and enabled them to distribute uniformly on the surface of the GO sheets. Furthermore, the Fe<sub>3</sub>O<sub>4</sub>@GO composite showed efficient catalytic activity for the reduction of nitroarenes. The yield of the reduction of nitrobenzene reached up to 99.2% after 18 min with Fe<sub>3</sub>O<sub>4</sub>@GO (3.1 wt%) being used as catalyst. The Fe<sub>3</sub>O<sub>4</sub>@GO composite offers significant advantages, such as low dosage, high catalytic activity, easy recycling and excellent stability, indicating that using graphene as a host material for catalysts to accomplish synthetic transformations has great potential and far-reaching prospects for industrial application.

## Acknowledgments

The financial supports from the National Natural Science Foundation of China (51202020), the International Science and Technology Cooperation Program of Changzhou City (CZ20110022), the Science and Technology Department of Jiangsu Province (BY2012099), the Qing Lan Project of Jiangsu Province and the Priority Academic Program Development of Jiangsu Higher Education Institutions are gratefully acknowledged.

## Appendix A. Supplementary data

Supplementary data associated with this article can be found, in the online version, at <http://dx.doi.org/10.1016/j.materresbull.2013.01.038>.

## References

- [1] R.S. Downing, P.J. Kunkeler, H. van Bekkum, *Catal. Today* 37 (1997) 121–136.
- [2] A.J. Béchamp, *Anal. Chim. Phys.* 42 (1854) 186.
- [3] N. Zinin, *J. Prakt. Chem.* 27 (1842) 140–153.
- [4] M. Takasaki, Y. Motoyama, K. Higashi, S.H. Yoon, I. Mochida, H. Nagashima, *Org. Lett.* 10 (2008) 1601–1604.
- [5] Y.Y. Chen, J.S. Qiu, X.K. Wang, J.H. Xiu, *J. Catal.* 242 (2006) 227–230.

- [6] I.M.J. Vilella, S.R. de Miguel, O.A. Scelza, *Chem. Eng. J.* 114 (2005) 33–38.
- [7] H. Wu, L.M. Zhuo, Q. He, X.P. Liao, B. Shi, *Appl. Catal. A* 366 (2009) 44–56.
- [8] M.V. Rajashekharan, D.D. Nikalje, R. Jaganathan, R.V. Chaudhari, *Ind. Eng. Chem. Res.* 36 (1997) 592–604.
- [9] J. Hine, S. Hahn, D.E. Miles, K. Ahn, *J. Org. Chem.* 50 (1985) 5092–5096.
- [10] T. Miyata, Y. Ishino, T. Hirashima, *Synthesis* (1978) 834–835.
- [11] M. Lauwiner, P. Rys, J. Wissmann, *Appl. Catal. A* 172 (1998) 141–148.
- [12] U. Sharma, P.K. Verma, N. Kumar, V. Kumar, M. Bala, B. Singh, *Chem. Eur. J.* 17 (2011) 5903–5907.
- [13] R.V. Jagadeesh, G. Wienhofer, F.A. Westerhaus, A. Surkus, M. Pohl, H. Junge, K. Junge, M. Beller, *Chem. Commun.* 47 (2011) 10972–10974.
- [14] Q.X. Shi, R.W. Lu, L.H. Lu, X.M. Fu, D.F. Zhao, *Adv. Synth. Catal.* 349 (2007) 1877–1881.
- [15] Y. Jang, S. Kim, S.W. Jun, B.H. Kim, S. Hwang, I.K. Song, B.M. Kim, T. Hyeon, *Chem. Commun.* 47 (2011) 3601–3603.
- [16] S. Kim, E. Kim, B.M. Kim, *Chem. Asian J.* 6 (2011) 1921–1925.
- [17] Y.S. Fu, H.Q. Chen, X.Q. Sun, X. Wang, *Appl. Catal. B* 111 (2012) 280–287.
- [18] Y.S. Fu, X. Wang, *Ind. Eng. Chem. Res.* 50 (2011) 7210–7218.
- [19] W.S. Hummers, R.E. Offeman, *J. Am. Chem. Soc.* 80 (1958) 1339.
- [20] N.I. Kovtyukhova, P.J. Ollivier, B.R. Martin, T.E. Mallouk, S.A. Chizhik, E.V. Buza-neva, A.D. Gorchinskiy, *Chem. Mater.* 11 (1999) 771–778.
- [21] H.Q. Chen, M.B. Müller, K.J. Gilmore, G.G. Wallace, D. Li, *Adv. Mater.* 20 (2008) 3557–3561.
- [22] G.Y. He, H.Q. Chen, J.W. Zhu, F.L. Bei, X.Q. Sun, X. Wang, *J. Mater. Chem.* 21 (2011) 14631–14638.
- [23] M.Z. Kassae, E. Motamedi, M. Majdi, *Chem. Eng. J.* 172 (2011) 540–549.
- [24] Y.H. Zhang, Z.R. Tang, X.Z. Fu, Y.J. Xu, *ACS Nano* 4 (2010) 7303–7314.
- [25] P.S. Kumbhar, J. Sanehez-Valente, F. Figueras, *Tetrahedron Lett.* 39 (1998) 2573–2574.
- [26] E.J. Corey, D.J. Pasto, W.L. Mock, *J. Am. Chem. Soc.* 83 (1961) 2957–2958.
- [27] J.W. Larsen, M. Freund, K.Y. Kim, M. Sidovar, J.L. Stuart, *Carbon* 38 (2000) 655–661.
- [28] P.S. Kumbhar, J. Sanchez-Valente, J.M.M. Millet, F. Figueras, *J. Catal.* 191 (2000) 467–473.
- [29] Y.J. Gao, D. Ma, C.L. Wang, J. Guan, X.H. Bao, *Chem. Commun.* 47 (2011) 2432–2434.